

Article

The Wetting Characteristics and Microscopic Wetting Mechanism of Coal under High-Pressure Nitrogen Environment

Piao Long ¹, Bin Shi ^{1,2,3,4,5,*}, Yunxing Cao ^{1,2,3,4,5,*}, Yufei Qi ¹, Xinyi Chen ¹ and Liuyang Li ¹

¹ School of Resources and Environment, Henan Polytechnic University, Jiaozuo 454000, China; lopo228@163.com (P.L.); lly040399@163.com (L.L.)

² Henan International Joint Laboratory for Unconventional Energy Geology and Development, Henan Polytechnic University, Jiaozuo 454000, China

³ Gas Geology and Engineering Research Center, Henan Polytechnic University, Jiaozuo 454000, China

⁴ Collaborative Innovation Center of Coal Work Safety and Clean High Efficiency Utilization, Henan Polytechnic University, Jiaozuo 454000, China

⁵ Collaborative Innovation Center of Coalbed Methane and Shale Gas for Central Plains Economic Region, Henan Polytechnic University, Jiaozuo 454000, China

* Correspondence: shibinwen-ls@163.com (B.S.); yxcao17@126.com (Y.C.)

Abstract: The wettability of coal is an important factor influencing hydraulic stimulation. Field-trial data has proven that high-pressure N₂ injection plays a positive role in increasing the coalbed methane (CBM) production rate. For the purpose of investigating the mechanism by which N₂ promotes the gas rate, multiple experiments were conducted sequentially on the wettability of anthracite under different N₂ pressures. Testing of the coal surface contact angle was conducted under 0.1–8 MPa nitrogen pressure using a newly built contact angle measuring device. The coal samples were collected from the Xinjing Coal Mine in the Qinshui Basin, China. The test results revealed that the contact angle increased with increasing N₂ pressure. That is, the contact angle was 77.9° at an N₂ pressure of 0.1 MPa and gradually increased to 101.4° at an infinite N₂ pressure. In contrast, the capillary pressure decreased with an increasing N₂ pressure, from 0.298 MPa to −0.281 MPa. The relationship between contact angle and N₂ pressure indicated that the wettability was reversed at a N₂ pressure of 5.26 MPa, with a contact angle of 90° and a capillary pressure of 0 MPa. The capillary pressure reversed to a negative value as the N₂ pressure increased. At the microlevel, a high N₂ pressure increases the surface roughness of coal, which improves the ability of the coal matrix to adsorb N₂, forming the gas barrier that hinders the intrusion of water into the pores of the coal matrix. The results of this study provide laboratory evidence that high-pressure N₂ injection can prevent water contamination and reduce the capillary pressure, thus benefiting coalbed methane production.

Keywords: coalbed methane; contact angle; capillary pressure; wettability; surface roughness



Citation: Long, P.; Shi, B.; Cao, Y.; Qi, Y.; Chen, X.; Li, L. The Wetting Characteristics and Microscopic Wetting Mechanism of Coal under High-Pressure Nitrogen Environment. *Processes* **2024**, *12*, 568. <https://doi.org/10.3390/pr12030568>

Academic Editor: Carlos Sierra Fernández

Received: 20 February 2024

Revised: 8 March 2024

Accepted: 11 March 2024

Published: 13 March 2024



Copyright: © 2024 by the authors. Licensee MDPI, Basel, Switzerland. This article is an open access article distributed under the terms and conditions of the Creative Commons Attribution (CC BY) license (<https://creativecommons.org/licenses/by/4.0/>).

1. Introduction

CBM is a type of clean and unconventional natural gas that holds immense significance in its development and utilization. It offers significant contributions in supplying clean energy, mitigating coal-mine gas disasters, and reducing carbon emissions [1–4]. Permeability plays a crucial role in evaluating the production potential of CBM wells [5–7]. Low-permeability coal seams are widely developed in China, accounting for 72%, and have been incentivized for a long time in the CBM industry [8–10].

Hydraulic fracturing has obvious advantages in improving the permeability of coal reservoirs and CBM production and has been widely used worldwide [11–13]. However, during high-pressure hydraulic fracturing, water intrusion into the pores of the coal matrix increases the capillary pressure, leading to capillary trapping or the water-blocking effect, inhibiting the transportation of CBM and reducing the recovery rate [14–17]. Contact

angle is one of the important parameters for characterizing wettability. The smaller the contact angle is, the better the wettability of the coal surface. On the contrary, the larger the contact angle is, the worse the wettability of the coal surface. In order to reduce the degree of inhibition of CBM desorption via hydraulic fracturing, increasing the coal–water contact angle by adding surfactants to the fracturing fluid is widely used in CBM well fracturing [18–20]. The liquid phase plays a certain role in affecting the contact angle of the coal surface, but the contact angle is more widely related to the properties of the solid phase, liquid phase, and gas phase. Among them, both solid and gas phases are key factors affecting the contact angle of the coal surface.

The surface roughness of coal (a solid property) is another factor determining the coal–water contact angle [21–23]. Shojai Kaveh et al. [24] investigated the wettability and surface roughness of hvbB coal under different CO₂ pressure atmospheres and found that, with an increase in CO₂ pressure, the surface roughness of coal increased because of the expansion of the coal matrix as a result of the diffusion of CO₂ into the coal matrix. Consequently, the contact angle increased. Song et al. [25] used atomic force microscopy (AFM) to study and analyze the relationship between the surface roughness and wettability of middle-order coal. It was found that increased roughness led to poorer wettability. The same results were also obtained for different coal ranks in a similar study [26].

The gas phase is another important factor affecting contact angle. Arif et al. [27] tested the contact angles of different coal rank samples under CO₂ pressures of 0–20 MPa and found that the contact angles of the different coal ranks increased with an increasing CO₂ pressure. A research group tested the coal–water contact angles of different-rank coal under CH₄, N₂, CO₂, and He pressures of 0–2 MPa [28–30]. They found that, as the gas pressure increased, the contact angles all increased, the higher the coal rank, the stronger the gas adsorption and the greater the increase in contact angle. The gas adsorption strengths were as follows: CO₂ > CH₄ > N₂ > He. It can be found that, in a gaseous environment, the contact angle increases with the increasing gas pressure, and the increasing trends of adsorbent gases are larger than those of non-adsorbent gases.

High-pressure N₂ is a common gaseous medium used for fracturing and production enhancement in low-permeability and low-pressure coal reservoirs because it has as low viscosity, strong penetration ability, and significant fracturing and permeability enhancement effects [23,31,32]. When its high expansion energy is released, it has the effects of driving the flow of the water in the coal seam, reducing the degree of water intrusion in the reservoir, and alleviating the damage of water to the reservoir [33,34]. Zhu et al. [35] conducted contact angle experiments on three coal samples under different N₂ pressures and found that the wettability worsens with an increasing N₂ pressure, and the highest rate of CBM production was related to the N₂ pressure. The field-test results of Cao [36] and Ni [37] showed that the injection of high-pressure N₂ into coal beds can increase CBM production. Therefore, an in-depth exploration of the contact angle properties under a high-pressure N₂ atmosphere is necessary.

Previous studies have indicated that injecting high-pressure N₂ into coal seams can increase the contact angle, eliminate the water-blocking effect, and increase CBM production. In engineering practice, engineers use a simple model to evaluate the change characteristics of the contact angle under N₂ injection to optimize the engineering design, but this model is currently unclear. Therefore, in this study, a high N₂ pressure environment contact angle measurement device was developed, a calculation model for the contact angle of anthracite under different N₂ pressures was established, and the trend of contact angle was analyzed. The changes in the coal surface roughness with and without N₂ treatment were tested and the influencing factors of the coal wetting characteristics under high N₂ pressures were explained from a microscopic perspective to provide theoretical guidance for the improvement of the CBM recovery rate via high N₂ pressure treatment.

2. Coal Samples and Laboratory Experiments

2.1. Sample Collection and Preparation

The coal samples were collected from coal seam 3# (Figure 1) in the Shanxi Formation (P_{1sh}) of the Xinjing Coal Mine, located in the northern Qinshui Basin, Shanxi Province, China. The thickness of this coal seam is 0.755–4.31 m, with an average of 2.33 m. The methane content is $18.17 \text{ m}^3/\text{t}$, and the permeability is 0.00047–0.00344 mD. And, it has a simple structure. Disturbed by tectonic deformation, fragmented coal and mylonite coal are well developed. Fresh block samples collected from the working face were immediately sealed with foil to prevent oxidation and moisture loss and were transported to the laboratory for cutting and crushing in preparation for subsequent testing. According to the relevant national standards [38–40], approximate analysis, elemental analysis, and mineral composition and density testing were conducted on the coal samples (Tables 1 and 2). The coal rank was classified as anthracite, indicated by the reflectance of 2.45% and volatile content of 11.06%. The mineral is mainly kaolinite, with a content of 70%. The true density is $1.67 \text{ g}/\text{cm}^3$, and the apparent density is $1.34 \text{ g}/\text{cm}^3$.

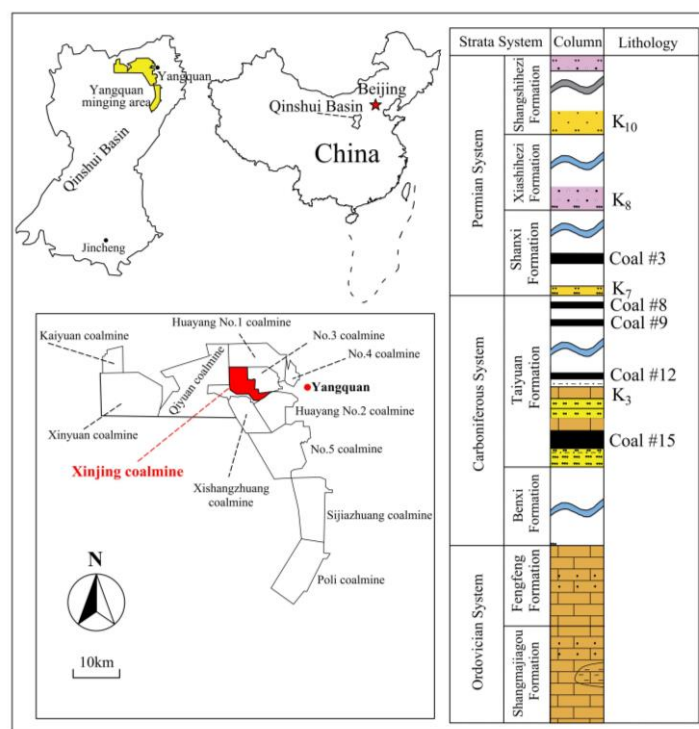


Figure 1. Geologic and stratigraphic maps of the Xinjing Coal Mine.

Table 1. Basic parameters of the coal samples.

Proximate Analysis (%)				Element Analysis (%)				$R_{o,max}$ (%)
M_{ad}	A_{ad}	V_{ad}	FC_{ad}	C_{daf}	H_{daf}	O_{daf}	N_{daf}	
1.00	15.74	11.06	72.20	91.52	3.95	3.05	1.11	2.46

Note: M : moisture content; A : ash yield; V : volatile matter; FC : fixed carbon; C : carbon; H : hydrogen; O : oxygen; N : nitrogen; ad : air-dry basis; daf : dry ash-free basis; $R_{o,max}$: maximum vitrinite reflectance.

Table 2. Mineral composition and density of coal samples.

Minerals (%)			Density (g/cm^3)	
Kaolinite	Quartz	Boehmite	True Density	Apparent Density
70	23.8	6.2	1.67	1.34

2.2. Contact Angle Experiment under Gas Atmosphere

To test the wettability of the coal under different N_2 pressure environments, a contact angle measurement platform was developed based on the German KRÜSS Drop Shape Analyzer DSA 25 (Figure 2). The platform was newly constructed by adding four units, including ① a high-pressure chamber made of transparent glass to allow clear observation of the water drops for accurate contact angle testing, which was the key component; ② a gas-injection system for injecting gas into the pressure chamber; ③ a manual water-injection pump; and ④ a sample adjustment system for conducting multiple measurements of one sample by adjusting the sample position. This platform can achieve contact angle testing under a gas atmosphere with pressures of 0–10 MPa, and the measurement range of the contact angle is 0–180°, with an accuracy of 0.1° (Table 2). The specific test steps are described below.

- (1) Make two cake-shaped coal samples (40 mm in diameter and 5 mm in thick). Use 240, 600, 1000, and 2000 mesh sandpaper to polish the samples until the surface is smooth and free of particle sensation. Finally, remove the residual powders on the surface of the samples using high-purity N_2 ;
- (2) Place the sample in the high-pressure transparent chamber and adjust the sample position, such that it can be observed through a camera. Turn on the gas-injection system to inject N_2 with a preset pressure and maintain this pressure for 4 h to allow the N_2 and coal samples to fully interact;
- (3) Slowly rotate the water-injection pump to drip distilled water onto the coal surface, record the water droplet on the coal surface using a high-definition camera to measure, and calculate the contact angle using a computer testing system;
- (4) Considering the nonuniformity of the coal surface, drop five drops and conduct measurements at different positions on the coal sample and take the average value as the contact angle of the sample;
- (5) Once step 4 is completed, remove the sample and allow it to dry. Then, repeat steps 1–4 to test the coal-water contact angle under different N_2 pressures of 1, 2, 3, 4, 5, 6, 7, and 8 MPa at a temperature of 20 °C.

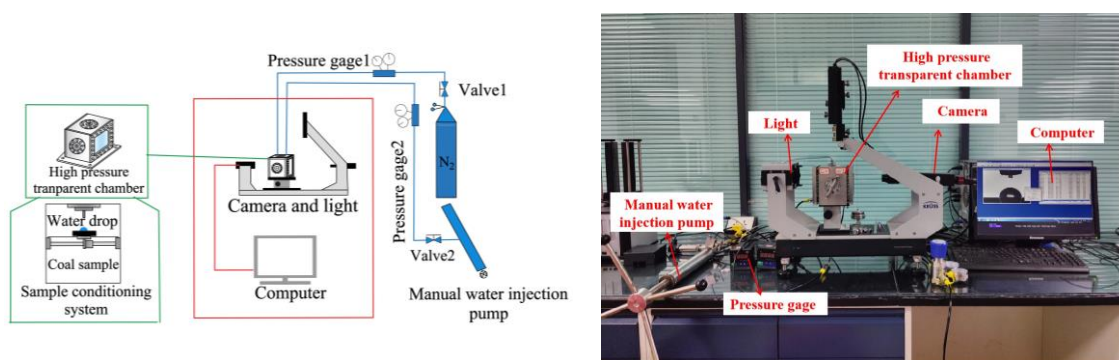


Figure 2. Diagram of contact angle testing device in pressured N_2 atmosphere.

2.3. Surface Roughness

The roughness of coal can affect the spreading ability and interaction forces of liquids on the surface of the coal [41]. According to the national standard GB/T 40066-2021 [42], AFM testing was performed on two coal samples that had undergone contact angle testing using the German Bruker Dimension Icon atomic microscope. The instrument can measure material properties at the nanoscale and compare the surface-roughness differences between N_2 -treated and non- N_2 -treated coal samples at the nanoscale. Finally, NanoScopeAnalysis1.9 software was used for 2D and 3D analysis of the coal surface.

3. Results and Analysis

3.1. Coal–Water Contact Angle

Figure 3 presents the test images of the coal–water contact angle under N_2 pressures from 0.1 MPa to 8.0 MPa. The measured contact angle under a pressure of 0.1 MPa was 77.9° . As the N_2 pressure increased from 1.0 MPa to 8.0 MPa, the contact angle gradually increased from 83.0° to 92.3° . In this study, the contact angle was the greatest (92.3°) under the designed N_2 pressure of 8.0 MPa and was 14.4° greater than that of 0.1 MPa. Wettability changed from water–wetness (contact angle $< 90^\circ$) to gas–wetness (contact angle $> 90^\circ$). Within the N_2 pressure range of 0 to 5 MPa, the contact angle increased greatly. After 5 MPa, the increase gradually slowed down. It can be seen from Figure 3 that there was a N_2 pressure, within 5 to 6 MPa, at which the contact angle reached 90° , which is the water–gas reverse point.

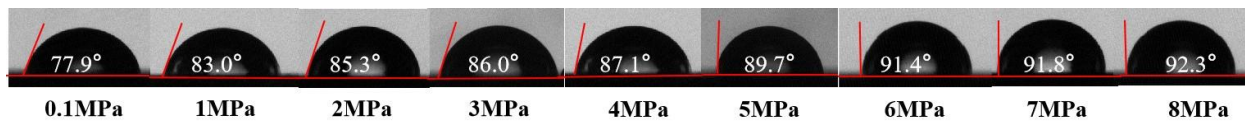


Figure 3. Photos showing the contact angles under different N_2 pressures.

3.2. Surface Roughness

The surface roughness of coal is related to its wettability characteristics. The higher the roughness, the worse its wettability. It has also been found that roughness is an indicator for evaluating the adsorption capacity of coal. The larger the roughness, the more adsorption points present on the coal, and the stronger the adsorption capacity [43]. Figure 4 shows the two- and three-dimensional morphology of the coal surface. The colors in Figure 4 represent the relative elevations or different degrees of height and undulation. The lighter the color, the higher the relative elevation; the darker the color, the lower the relative elevation.

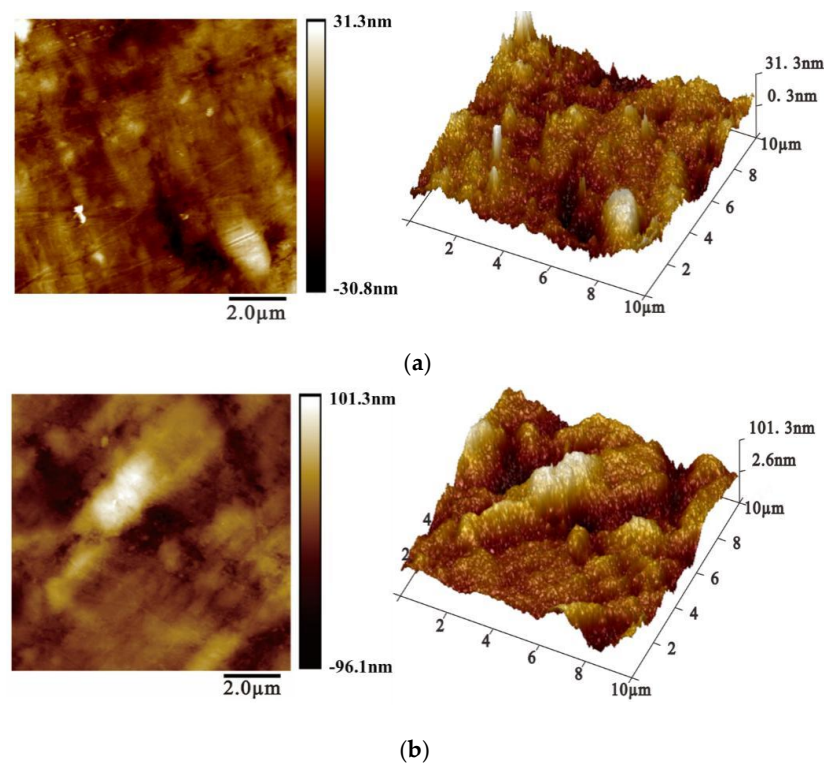


Figure 4. AFM images in 2D and 3D of coal samples with and without N_2 treatment. (a) AFM Images of coal without N_2 treatment. (b) AFM Images of coal with N_2 treatment.

Figure 4a presents an AFM image of the sample without N₂ treatment. Its surface has small particle clusters with relatively sharp and steep peaks. The relative elevations of the low caves and high peaks range from −30.8 to 31.3 nm, with an elevation difference of 62.1 nm, and the calculated average roughness is 5.6 nm. Thus, the surface roughness of the sample without N₂ treatment is small. Figure 4b presents an AFM image of the sample subjected to N₂ treatment. The relative elevations of the low caves and high peaks range from −96.1 to 101.3 nm, with a difference of 197.4 nm, and the calculated average roughness is 22.3 nm. The average roughness is 3.2 times greater after N₂ treatment (Table 3).

Table 3. Surface roughness of the coals with and without N₂ treatment.

Coal Sample	Maximum Fluctuation Height (nm)	Minimum Fluctuation Height (nm)	Roughness (nm)	Standard Deviation (nm)
Without N ₂ treatment	31.3	−30.8	5.6	0.28
Pressure N ₂ treated	101.3	−96.1	22.3	2.14

4. Discussion

4.1. Mathematical Relationship between Contact Angle and N₂ Pressure

To determine how the contact angle varies with increasing N₂ pressure, as well as the water–gas wettability reverse point, a mathematical relationship between the contact angle and N₂ pressure was determined (Figure 5 and Equation (1)). The fitting coefficient R² is 0.97, indicating a high degree of confidence. the coal–water contact angle in the N₂ atmosphere (°) is θ , and P is the nitrogen pressure (MPa).

$$\theta = \frac{abP}{1 + bP} + c \quad (1)$$

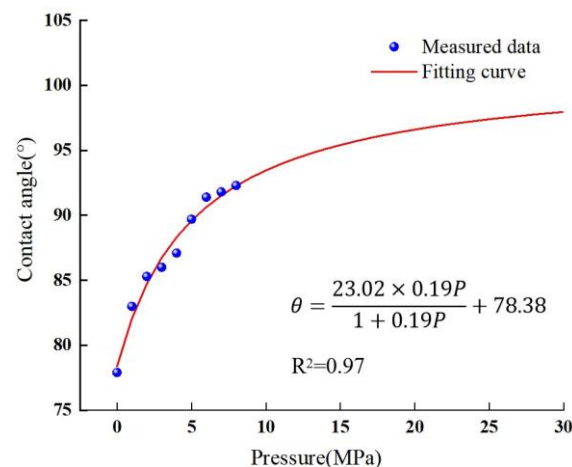


Figure 5. Contact angle versus N₂ pressure.

a is the theoretical maximum contact angle increment under whatever high N₂ pressure atmosphere (°), which is related to the adsorption capacity of a specific coal rank. In this study, the theoretical value of a is 23.02° in a N₂ atmosphere for Xinjing’s anthracite coal. In the case of a CO₂ and CH₄ gas atmosphere, the a value of the studied coal samples will increase because the adsorption capacities of CO₂ and CH₄ are stronger than that of N₂.

b is the reciprocal of the N₂ pressure when the wettability undergoes a reversal (MPa^{−1}). In this study, the b value of the anthracite coal is 0.19 (Table 4 and Figure 5). It is an indicator for evaluating the difficulty of the wettability reversal of a coal sample. The higher the value of b , the easier the wettability reversal. The theoretical N₂ pressure of the wettability reversal is 5.26 MPa for the studied coal sample.

c is the theoretical initial contact angle under standard atmospheric pressure of 0.1 MPa ($^{\circ}$). The c value of the studied coal sample is 78.38° , which is consistent with the measured value of 77.90° .

Table 4. Key parameters in Equation (1) for the studied coal.

a ($^{\circ}$)	b (MPa $^{-1}$)	c ($^{\circ}$)	R^2
23.02	0.19	78.38	0.97

It should be noted that Equation (1) is similar to the Langmuir equation, a mathematical expression of the isothermal adsorption mechanism. The increase in coal–water contact angle, induced by N_2 , is mainly caused by the pressure of N_2 occupying more adsorption sites, which finally hinders the water molecules from intruding into the pores of the coal matrix.

In this study of anthracite coal, Equation (1) can be written as follows:

$$\theta = \frac{23.02 \times 0.19P}{1 + 0.19P} + 78.38 \quad (2)$$

Using the above equation, we can evaluate or predict the contact angle variation range in different N_2 pressure environments, providing CBM engineers with a high confidence in determining the N_2 injection design. However, for different coalification ranks, the values of a , b , and c will be different and can be obtained via laboratory experiments.

Although the contact angle has been studied under pressured-gas conditions for a long time, the mathematical expression in Equation (1) is addressed for the first time in this study [24,30,44].

4.2. Capillary Pressure Changes Induced by Contact Angle and N_2 Pressure

CBM engineers must reduce the water pressure inside the matrix pores and fractures to below the critical desorption pressure through water drainage, resulting in the desorption and production of CBM. The magnitude and direction of the capillary pressure of the matrix pores have a significant impact on the migration ability of CBM [45]. When the capillary pressure is positive, it resists and hinders the migration of CBM. The greater the capillary pressure, the greater the resistance, and the more difficult is the gas migration. When the capillary pressure is reversed to negative, it transforms into the driving force and promotes the migration of CBM [46,47]. The smaller the capillary pressure is, the greater the driving force.

The magnitude of the capillary pressure can be expressed by the Laplace formula:

$$P_c = \frac{2\sigma\cos\theta}{r_c} \quad (3)$$

where P_c is the capillary pressure (MPa); σ is the surface tension (mN/m); θ is the contact angle ($^{\circ}$); and r_c is the capillary radius (nm).

According to the decimal coal pore classification scheme [48], <10 nm pores are adsorption pores, 10–100 nm pores are diffusion pores, and >100 nm pores are seepage pores. Therefore, the capillary pressure of the studied coal is calculated based on the contact angle obtained from the experimental testing (0.1–8 MPa) and Equation (1). The r_c and surface tension σ , of the water are determined to be 100 nm and 71.2 mN/m. According to Equation (3), the capillary pressures under different N_2 pressures are calculated (Table 5 and Figure 6).

Table 5. Capillary pressures for various contact angles and N₂ pressures.

Contact Angle Source	N ₂ Pressure (MPa)	Contact Angle (°)	Capillary Pressure (MPa)
Actual measurement	0.1	77.9	0.298
	1	83.0	0.174
	2	85.3	0.117
	3	86.0	0.099
	4	87.1	0.554
	5	89.7	0.007
	6	91.4	−0.035
	7	91.8	−0.045
Fitted	8	92.3	−0.057
	10	93.5	−0.086
	15	95.4	−0.135
	20	96.6	−0.164
	25	97.4	−0.183
	30	98.0	−0.197
	35	98.4	−0.208
	40	98.7	−0.216
	∞	101.4	−0.281

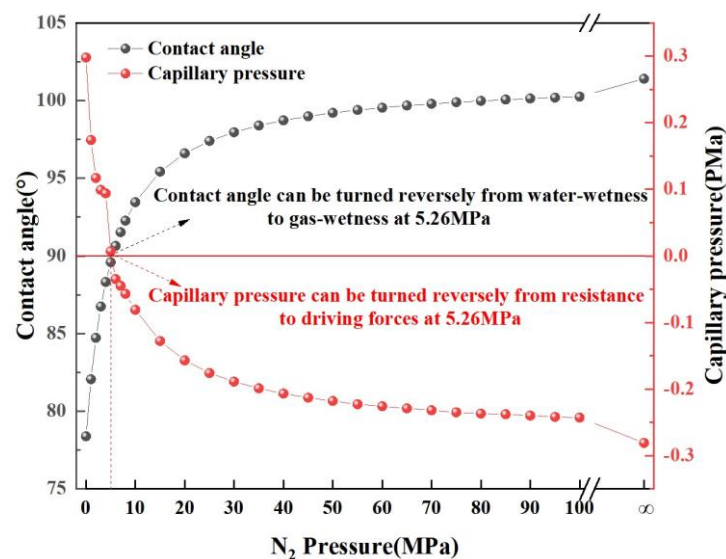
**Figure 6.** Capillary pressure and contact angle versus N₂ pressure.

Figure 6 shows that as the N₂ pressure increases, the contact angle gradually increases, and the capillary pressure gradually decreases. Under a high-pressure N₂ atmosphere, the theoretical maximum contact angle of the experimental coal sample increases to 101.4°, and the theoretical minimum capillary pressure decreases to −0.281 MPa. When the N₂ pressure reaches 5.26 MPa, the contact angle is 90°, and the capillary pressure is 0 MPa.

Thus, we define 5.26 MPa as the critical N₂ pressure for the studied coal, at which the wettability is reversed and the capillary pressure changes from a resisting force to a driving force. When the N₂ pressure is less than 5.26 MPa, the contact angle is less than 90°, and the capillary pressure is positive. The capillary pressure is directed from the liquid phase to the gas phase (Figure 7a), providing resistance and hindering CBM migration or sealing the CBM in the pores and fractures. This phenomenon is defined as the water-blocking effect. When the N₂ pressure is greater than 5.26 MPa, the contact angle is greater than 90°, which causes the capillary pressure to be negative, and, finally, the capillary force reverses from the gas phase to the liquid phase (Figure 7b). The capillary pressure changes from a resisting force to a driving force, driving the transportation of CBM within the coal matrix pores and fractures, which promotes more CBM production.

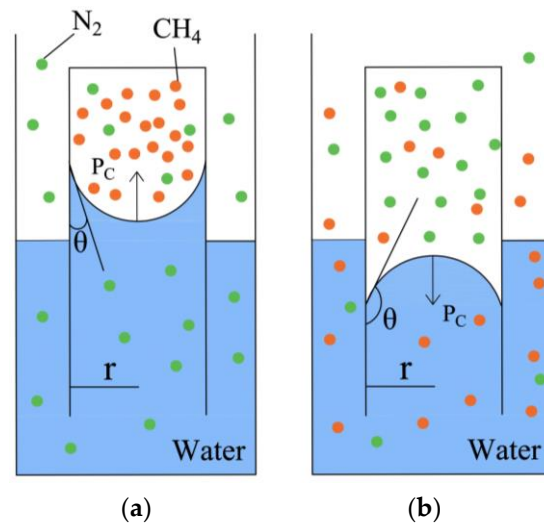


Figure 7. Changes in magnitude and direction of capillary pressure. (a) N_2 pressure < 5.26 MPa. (b) N_2 pressure > 5.26 MPa.

Coal is a porous material. Nanometer scale micropores, which are most easily water blocked under high-pressure hydraulic stimulation, account for 90% of the total pore volume. The water-blocking effect is a significant factor in reducing methane migration and production. Surfactant technology has been developed to eliminate the water-blocking effect in the CBM industry for a long time. But, it has a high cost, and the desired goal is not always reached. The new findings of this study provide a new measure for reducing the water-blocking effect, i.e., to efficiently develop coal reservoirs, i.e., injecting high-pressure N_2 .

4.3. Mechanism of Contact Angle/Capillary Pressure Reversal under N_2 Pressure

Under different gas atmospheres, such as CH_4 [28], CO_2 [27], and N_2 [35], as the gas pressure increases, the gas density inside the testing chamber also increases. The adsorption of gas molecules on the coal surface also increases, reducing the ability of water molecules to invade the coal matrix. This leads to an increasing contact angle and capillary pressure. When the contact angle is greater than 90° , the capillary pressure changes to a negative value. The roughness tests results for the coal samples with and without N_2 treatment obtained in this study provide a better understanding of the mechanism by which the competitive adsorption of N_2 and water affects the contact angle.

Competitive adsorption of N_2 and water occurs as follows. When the coal initially adsorbs a small amount of gas (Figure 8a), and as the pressure increases progressively, more and more adsorption sites in the coal are occupied by the gas. As the monolayer adsorption (Figure 8b) changes to multilayer adsorption (Figure 8c), a “gas barrier” forms on the surface of the coal. This “gas barrier” effectively hinders the intrusion of water molecules and increases the contact angle.

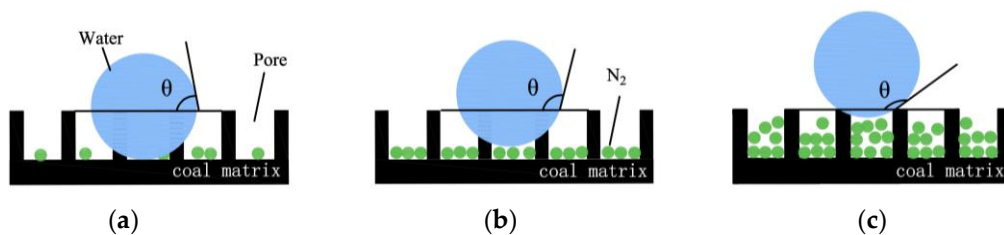


Figure 8. Changes in contact angle of coal surface before and after N_2 adsorption. (a) N_2 pressure of 0.1 MPa. (b) N_2 monolayer adsorption. (c) N_2 multi-monolayer adsorption.

Coal has a specific expanding–shrinking property. That is, it expands when gas is adsorbed and shrinks when gas is desorbed. The magnitude of coal expansion gradually increases as more gas is adsorbed in the coal, and we can use the surface roughness to describe the degree of expansion, i.e., the greater the roughness. The greater the expansion of the coal, the more gas is adsorbed.

The observations presented in Figure 4 and Table 3 reveal that the roughness of coal increased by 3.2 times after high-pressure N₂ (8.0 MPa) treatment. This high roughness is interpreted as the significant expansion of coal, as a large amount of N₂ is adsorbed under high pressure. Thus, the “gas barrier” with multilayer N₂ adsorption generated on the coal surface strongly hinders the intrusion of water into the coal matrix, causing the contact angle to increase and the capillary pressure to decrease, becoming even more negative.

5. Conclusions

For investigating the mechanism by which pressurized N₂ injection in a coal reservoir significantly improves CBM production, a series of coal–water contact angle experiments on anthracite samples were conducted under N₂ pressures of 0.1 to 8 MPa using a newly constructed testing platform. The surface roughness of samples with and without N₂ treatment was measured via AFM. The main conclusions of this study are as follows.

- (1) The contact angle of anthracite increases with the increase of N₂ pressure and finally stabilizes; the relationship between contact angle and N₂ pressure is similar to the Langmuir isothermal adsorption curve;
- (2) With the increase of N₂ pressure, the amount of N₂ adsorbed in the coal matrix increases, which is the main reason for the increase in contact angle. At 5.26 MPa N₂ pressure, the contact angle reaches 90°, and the wettability of anthracite is reversed. The capillary pressure changes from a resisting force to a driving force;
- (3) In addition, high-pressure N₂ increases the surface roughness of the coal matrix and enhances the adsorption capacity and amount of N₂, which is beneficial for improving the contact angle.

This research improves our understanding of why and how high-pressure N₂ stimulation can reduce the capillary pressure or alleviate the water-blocking effect in low-pressure coal reservoirs, and they provide an advanced measure with a high confidence of effectively increasing CBM production via high-pressure N₂ injection.

Author Contributions: P.L.: Methodology, Investigation, Data analysis, Writing—original draft and editing. B.S.: Methodology, Experimental guidance, Writing—review and editing. Y.C.: Conceptualization, Project administration, Funding acquisition, Supervision, Writing—review and editing. Y.Q.: Conceptualization, Methodology, Data analysis. X.C.: Investigation, Data analysis. L.L.: Conceptualization, Methodology, Writing and editing. All authors have read and agreed to the published version of the manuscript.

Funding: This work was financially supported by the key Program of the National Natural Science Foundation of China [42230814] and the unveiling projects of the Department of Science and Technology of Shanxi Province [20191101018].

Data Availability Statement: Data are contained within the article.

Conflicts of Interest: The authors declare that they have no known competing financial interests or personal relationships that could have appeared to influence the work reported in this paper.

References

1. Dávila-Pulido, G.I.; González-Ibarra, A.A.; Garza-García, M. A brief review on coal reserves, production and possible non-power uses: The case of Mexico. *Heliyon* **2023**, *9*, e16043. [[CrossRef](#)]
2. Wu, X.F.; Li, H.X.; Wang, B.L.; Zhu, M.B. Review on Improvements to the Safety Level of Coal Mines by Applying Intelligent Coal Mining. *Sustainability* **2022**, *14*, 16400. [[CrossRef](#)]
3. Xu, F.; Hou, W.; Xiong, X.; Xu, B.; Wu, P.; Wang, H.; Feng, K.; Yun, J.; Li, S.; Zhang, L.; et al. The status and development strategy of coalbed methane industry in China. *Pet. Explor. Dev.* **2023**, *50*, 765–783. [[CrossRef](#)]

4. Guo, Z.X.; Zhao, J.Z.; You, Z.J.; Li, Y.M.; Zhang, S.; Chen, Y.Y. Prediction of coalbed methane production based on deep learning. *Energy* **2021**, *230*, 120847. [[CrossRef](#)]
5. Li, J.; Li, B.; Pan, Z.; Wang, Z.; Yang, K.; Ren, C.; Xu, J. Coal Permeability Evolution Under Different Water-Bearing Conditions. *Nat. Resour. Res.* **2020**, *29*, 2451–2465. [[CrossRef](#)]
6. Lu, Y.; Meng, Z.; Su, X.; Yu, Y. Experimental Study of Dynamic Permeability Changes in Coals of Various Ranks During Hydraulic Fracturing. *Nat. Resour. Res.* **2022**, *31*, 3253–3272. [[CrossRef](#)]
7. Yu, Y.; Meng, Z.; Gao, C.; Lu, Y.; Li, J. Experimental Investigation of Pore Pressure Effect on Coal Sample Permeability Under Different Temperatures. *Nat. Resour. Res.* **2022**, *31*, 1585–1599. [[CrossRef](#)]
8. Zhou, L.; Zhou, X.; Fan, C.; Bai, G. Coal permeability evolution triggered by variable injection parameters during gas mixture enhanced methane recovery. *Energy* **2022**, *252*, 124065. [[CrossRef](#)]
9. Oudinot, A.Y.; Riestenberg, D.E.; Koperna, G.J. Enhanced Gas Recovery and CO₂ Storage in Coal Bed Methane Reservoirs with N₂ Co-Injection. *Energy Procedia* **2017**, *114*, 5356–5376. [[CrossRef](#)]
10. Kang, Y.; Sun, L.; Zhang, B.; Jiaoyang, G.; Delei, M. Discussion on classification of coalbed reservoir permeability in China. *J. China Coal Soc.* **2017**, *42* (Suppl. S1), 186–194.
11. Cao, W.; Yildirim, B.; Durucan, S.; Wolf, K.-H.; Cai, W.; Agrawal, H.; Korre, A. Fracture behaviour and seismic response of naturally fractured coal subjected to true triaxial stresses and hydraulic fracturing. *Fuel* **2021**, *288*, 119618. [[CrossRef](#)]
12. Li, H.; Liang, W.; Jiang, Y.; Wu, P.; Wu, J.; He, W. Numerical Study on the Field-Scale Criterion of Hydraulic Fracture Crossing the Interface Between Roof and Broken Low-Permeability Coal. *Rock Mech. Rock Eng.* **2021**, *54*, 4543–4567. [[CrossRef](#)]
13. Zhang, B.; Li, B.; Zhang, D.; Li, J. Experimental research on permeability variation from the process of hydraulic fracturing of high-rank coal. *Environ. Earth Sci.* **2020**, *79*, 45. [[CrossRef](#)]
14. Yang, L.; Ge, H.K.; Shi, X.; Li, J.; Zhou, T.; Cao, W.K.; Zhang, K.H.; Zhang, Y.J.; Gao, M. Experimental and numerical study on the relationship between water imbibition and salt ion diffusion in fractured shale reservoirs. *J. Nat. Gas Sci. Eng.* **2017**, *38*, 283–297. [[CrossRef](#)]
15. Liu, Q.; Nie, W.; Hua, Y.; Peng, H.; Liu, Z. The effects of the installation position of a multi-radial swirling air-curtain generator on dust diffusion and pollution rules in a fully-mechanized excavation face: A case study. *Powder Technol.* **2018**, *329*, 371–385. [[CrossRef](#)]
16. Plug, W.-J.; Mazumder, S.; Bruining, J. Capillary Pressure and Wettability Behavior of CO₂ Sequestration in Coal at Elevated Pressures. *SPE J.* **2008**, *13*, 455–464. [[CrossRef](#)]
17. Zhu, S.Y.; Peng, X.L.; You, Z.J.; Li, C.L.; Deng, P. The effects of cross-formational water flow on production in coal seam gas reservoir: A case study of Qinshui Basin in China. *J. Pet. Sci. Eng.* **2020**, *194*, 107516. [[CrossRef](#)]
18. Franco-Aguirre, M.; Zabala, R.D.; Lopera, S.H.; Franco, C.A.; Cortés, F.B. Interaction of anionic surfactant-nanoparticles for gas—Wettability alteration of sandstone in tight gas-condensate reservoirs. *J. Nat. Gas Sci. Eng.* **2018**, *51*, 53–64. [[CrossRef](#)]
19. Jia, L.; Li, K.; Shi, X.; Zhao, L.; Linghu, J. Application of gas wettability alteration to improve methane drainage performance: A case study. *Int. J. Min. Sci. Technol.* **2021**, *31*, 621–629. [[CrossRef](#)]
20. Liu, J.; Yang, T.; Yuan, J.; Chen, X.; Wang, L. Study on Eliminating the Water Blocking Effect in Coal Seams Using Gas-Wetting Reversal Technology. *ACS Omega* **2020**, *5*, 30687–30695. [[CrossRef](#)]
21. Li, C.; Zhang, J.; Han, J.; Yao, B.H. A numerical solution to the effects of surface roughness on water-coal contact angle. *Sci. Rep.* **2021**, *11*, 459. [[CrossRef](#)]
22. Yan, M.; Luo, H.; Yang, T.; Yan, D.; Wei, J.; Lin, H.; Li, S. Experimental Study on Fractal Characteristics of Surface Roughness of Briquettes and their Effect on Wettability of Coal Samples. *Nat. Resour. Res.* **2023**, *32*, 1235–1249. [[CrossRef](#)]
23. Zhang, B.; Fu, X.; Li, G.; Deng, Z.; Shen, Y.; Hao, M. An experimental study on the effect of nitrogen injection on the deformation of coal during methane desorption. *J. Nat. Gas Sci. Eng.* **2020**, *83*, 103529. [[CrossRef](#)]
24. Shojai Kaveh, N.; Rudolph, E.S.; Wolf, K.H.; Ashrafizadeh, S.N. Wettability determination by contact angle measurements: hvbB coal-water system with injection of synthetic flue gas and CO₂. *J. Colloid Interface Sci.* **2011**, *364*, 237–247. [[CrossRef](#)]
25. Song, L.; Song, Q.; Yan, J.; Shu, X. Study on wettability of coal dust based on its microtopography and surface free energy. *Coal Convers.* **2018**, *41*, 12–18.
26. Jia, C.; Lai, J.; Chen, W.; Lu, Y.; Cai, Y.; Liang, Y. Microscopic wettability of medium rank coals involved pore features and functional groups. *Nat. Gas Ind. B.* **2022**, *9*, 325–335. [[CrossRef](#)]
27. Arif, M.; Barifcani, A.; Lebedev, M.; Iglauer, S. CO₂-enhanced methane recovery. *Fuel* **2016**, *181*, 680–689. [[CrossRef](#)]
28. Wei, J.; Wang, H.; Si, L.; Xi, Y. Characteristics of coal-water solid-liquid contact in gas atmosphere. *J. China Coal Soc.* **2022**, *47*, 323–332.
29. Si, L.L.; Ding, N.; Wei, J.P.; Sheng, L.C.; Wang, L.; Li, Z.W.; Chen, X.M. Gas-liquid competitive adsorption characteristics and coal wetting mechanism under different pre-adsorbed gas conditions. *Fuel* **2022**, *329*, 125441. [[CrossRef](#)]
30. Ding, N.; Si, L.; Wei, J.; Jiang, W.; Zhang, J.; Liu, Y. Study on Coal Wettability under Different Gas Environments Based on the Adsorption Energy. *ACS Omega* **2023**, *8*, 22211–22222. [[CrossRef](#)]
31. Talapatra, A.; Halder, S.; Chowdhury, A.I. Enhancing coal bed methane recovery: Using injection of nitrogen and carbon dioxide mixture. *Pet. Sci. Technol.* **2021**, *39*, 49–62. [[CrossRef](#)]
32. Wang, Z.; Deng, Z.; Fu, X.; Li, G.; Pan, J.; Hao, M.; Zhou, H. Effects of Methane Saturation and Nitrogen Pressure on N₂-Enhanced Coalbed Methane Desorption Strain Characteristics of Medium-Rank Coal. *Nat. Resour. Res.* **2020**, *30*, 1527–1545. [[CrossRef](#)]

33. Yang, X.; Wang, G.; Ni, M.; Shu, L.; Gong, H.; Wang, Z. Investigation on Key Parameters of N₂ Injection to Enhance Coal Seam Gas Drainage (N₂-ECGD). *Energies* **2022**, *15*, 5064. [[CrossRef](#)]
34. Yang, X.; Wang, G.; Du, F.; Jin, L.; Gong, H. N₂ injection to enhance coal seam gas drainage (N₂-ECGD): Insights from underground field trial investigation. *Energy* **2022**, *239*, 122247. [[CrossRef](#)]
35. Zhu, Y.; Xing, H.; Rudolph, V.; Chen, Z. Quantifying the impact of capillary trapping on coal seam gas recovery. *J. Nat. Gas Sci. Eng.* **2020**, *83*, 103588. [[CrossRef](#)]
36. Cao, Y.; Shi, B.; Zhou, D.; Wu, H.; Liu, T.; Tian, L.; Cao, Y.; Jia, M. Study and application of stimulation technology for low production CBM well through high pressure N₂ Injection-soak. *J. China Coal Soc.* **2019**, *44*, 2556–2565.
37. Ni, X.; Jia, B.; Cao, Y. Study on Improving Coal-bed Gas Recovery Rate by Hydraulic Fracturing and Nitrogen Injection of Borehole. *Min. Saf. Environ. Prot.* **2012**, *39*, 1–3+6+7.
38. GB/T 212-2008; Proximate Analysis of Coal. Standards Press of China: Beijing, China, 2008.
39. GB/T 31391-2015; Ultimate Analysis of Coal. Standards Press of China: Beijing, China, 2015.
40. GB/T 6948-2008; Method of Determining Microscopically the Reflectance of Vitrinite in Coal. Standards Press of China: Beijing, China, 2008.
41. Zhang, J.; Xu, B.; Wei, J.; Zhang, P.; Cai, M.; Zhang, K. Numerical Simulation of Coal Surface Contact Angle Based on Roughness. *Coal Sci. Technol.* **2023**, *51*, 96–104.
42. GB/T 40066-2021; Nanotechnologies—Thickness Measurement of Graphene Oxide—Atomic Force Microscopy (AFM). Standards Press of China: Beijing, China, 2021.
43. Lu, Y.; Liu, D.; Cai, Y.; Gao, C.; Jia, Q.; Zhou, Y. AFM measurement of roughness, adhesive force and wettability in various rank coal samples from Qinshui and Junggar basin, China. *Fuel* **2022**, *317*, 123556. [[CrossRef](#)]
44. Arif, M.; Barifcani, A.; Iglauer, S. Solid/CO₂ and solid/water interfacial tensions as a function of pressure, temperature, salinity and mineral type: Implications for CO₂-wettability and CO₂ geo-storage. *Int. J. Greenh. Gas Control* **2016**, *53*, 263–273. [[CrossRef](#)]
45. Jia, L.; Li, K.; Zhou, J.; Yan, Z.; Wang, Y.; Mahlalela, B.M. Experimental study on enhancing coal-bed methane production by wettability alteration to gas wetness. *Fuel* **2019**, *255*, 115860. [[CrossRef](#)]
46. Wang, L.; Wang, B.; Zhu, J.T.; Liao, X.X.; Ni, S.J.; Shen, S.L. Experimental study on alleviating water-blocking effect and promoting coal gas desorption by gas wettability alteration. *J. Nat. Gas Sci. Eng.* **2022**, *108*, 104805. [[CrossRef](#)]
47. Sun, Z.; Li, X.; Liu, W.; Zhang, T.; He, M.; Nasrabadi, H. Molecular dynamics of methane flow behavior through realistic organic nanopores under geologic shale condition: Pore size and kerogen types. *Chem. Eng. J.* **2020**, *398*, 124341. [[CrossRef](#)]
48. Hu, B.; Cheng, Y.P.; Pan, Z.J. Classification methods of pore structures in coal: A review and new insight. *Gas Sci. Eng.* **2023**, *110*, 204876. [[CrossRef](#)]

Disclaimer/Publisher's Note: The statements, opinions and data contained in all publications are solely those of the individual author(s) and contributor(s) and not of MDPI and/or the editor(s). MDPI and/or the editor(s) disclaim responsibility for any injury to people or property resulting from any ideas, methods, instructions or products referred to in the content.